Predictive performance model for hydraulic flocculator design with polyaluminum chloride and aluminum sulfate coagulants

Karen A. Swetland, Monroe L. Weber-Shirk*, Leonard W. Lion

*Email: mw24@cornell.edu Phone: 1 607 216 8445 Fax: 1 607 255 9004

School of Civil and Environmental Engineering, Cornell University, Ithaca, NY 14853, USA

Abstract

Mechanistically-based scalable algorithms for design and operation of hydraulic flocculators were developed in this research based on observations of residual turbidity for a range of influent turbidities ($5-500\,NTU$) and coagulant doses ($0.01-0.15\,mM\,Al$), for two hydraulic residence times ($800\,s$ and $1200\,s$) and for two coagulant types (polyaluminum chloride and aluminum sulfate). Data were obtained over a range of sedimentation capture velocities using a bench-scale laminar flow tube flocculator and quiescent settling column. Seemingly disparate results were unified through creation of a composite design parameter that considers collision potential in the flocculator and coagulant surface coverage of colloids. One adjustable model parameter was used to fit data ($R^2 \approx 0.9$) from over 136 experiments to create a model for each of the two coagulants. The model is applicable over a range of sedimentation tank capture velocities and accurately reflects the effects of coagulant dose, raw water turbidity, flocculator residence time, and coagulant type. The model was validated by successfully predicting results from independent data sets. When calibrated properly to the coagulant and source water to be treated, the predictive model is expected to be a useful tool in the design and operation of hydraulic flocculators.

Keywords: Hydraulic flocculation, predictive model, laminar flow, alum, polyaluminum chloride (PACl), surface coverage, collision potential, turbidity removal

Contents

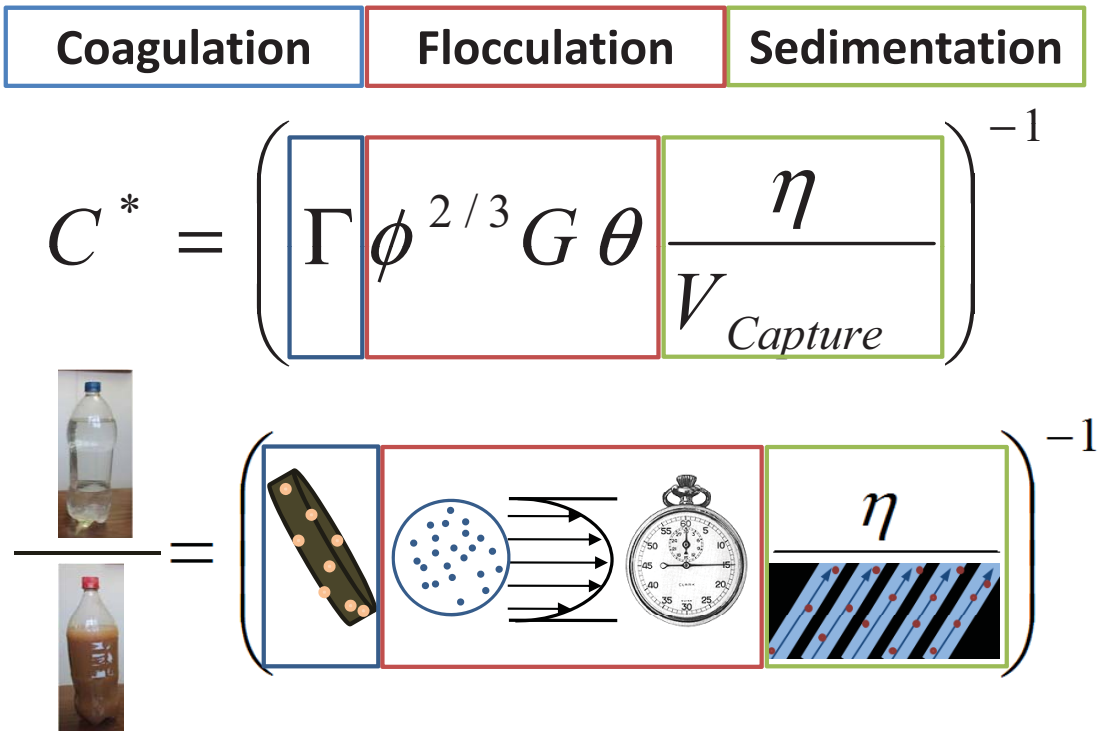

Introduction

One objective of flocculation research is to enhance the performance of flocculators in concert with subsequent unit processes (e.g., sedimentation and filtration) while minimizing overall construction and operation costs. Multiple variables influence the performance of hydraulic flocculators in drinking water treatment, including but not limited to: the concentration and type of colloids in the raw water, the concentration of dissolved organic matter, coagulant type and dose, and hydraulic residence time and energy dissipation rate in the flocculator (Kawamura, 1991). Quantifying the effect of varying flocculator design and operational parameters on the post-sedimentation residual turbidity that corresponds to a selected sedimentation tank capture velocity (often referred to as the critical velocity) is a necessary step in differentiating the role each of these parameters play in flocculator performance.

The design and operation of hydraulic flocculators (e.g., units where colloid transport and mixing are achieved by fluid flow rather than by mechanical means) would be aided by a predictive model that can characterize performance of alternative designs under reasonable operating conditions. A general model would be scalable and utilize dimensionally-correct relationships that are based upon relevant flocculation mechanisms. Existing design guidelines for flocculators are predominantly based on empiricism rather than a fundamental understanding of the underlying physical and chemical processes (Hendricks, 2006) and design guidelines for gravity-powered hydraulic flocculators are inadequate (Schulz and Okun, 1984). The evidence for empiricism can be seen in the use of guidelines that are not dimensionless and that cannot be easily made dimensionless. For example, in the Ten State Standards the guidance for the design of flocculator states "The flow through velocity should be not less than 0.5 nor greater than 1.5 feet per minuteThe Great Lakes - Upper Mississippi River Board of State and Provincial Public Health and Environmental Managers (2007)." It is well established that floc size is correlated with energy dissipation rate (not velocity) (Akers et al., 1987; Weber-Shirk and Lion, 2010; Cleasby, 1984) and thus, if the goal of these guidelines is to be able to deliver flocs of a certain size to the sedimentation tank, then the design specification should be a maximum energy dissipation rate. Since the relationship between energy dissipation rate and velocity is dependent on the scale of the flow, velocity guidelines result in design failure for small scale facilities. The pervasive lack of scalable design guidelines provides an opportunity for research to significantly improve conventional flocculator designs.

In this research a spectrum of coagulant doses (which control colloid surface coverage), and influent turbidities, were evaluated for two alternative coagulants and two hydraulic residence times with respect to their influence on floc settling properties (as manifested by residual turbidity) at multiple sedimentation capture velocities. The observations from these experiments are utilized to formulate a comprehensive model that is able to predict settled water turbidity as a function of flocculator design and operation for laminar flow tube flocculators.

Experimental Methods

Experiments were conducted using an apparatus comprised of synthetic raw water and coagulant metering systems, a coiled tube hydraulic flocculator, and a flocculation residual turbidity analyzer (FReTA) (see Figure 1). Tse et al. (2011) provide a complete description of the experimental apparatus and methods; only the length of the flocculator was changed for the experimental results presented here.

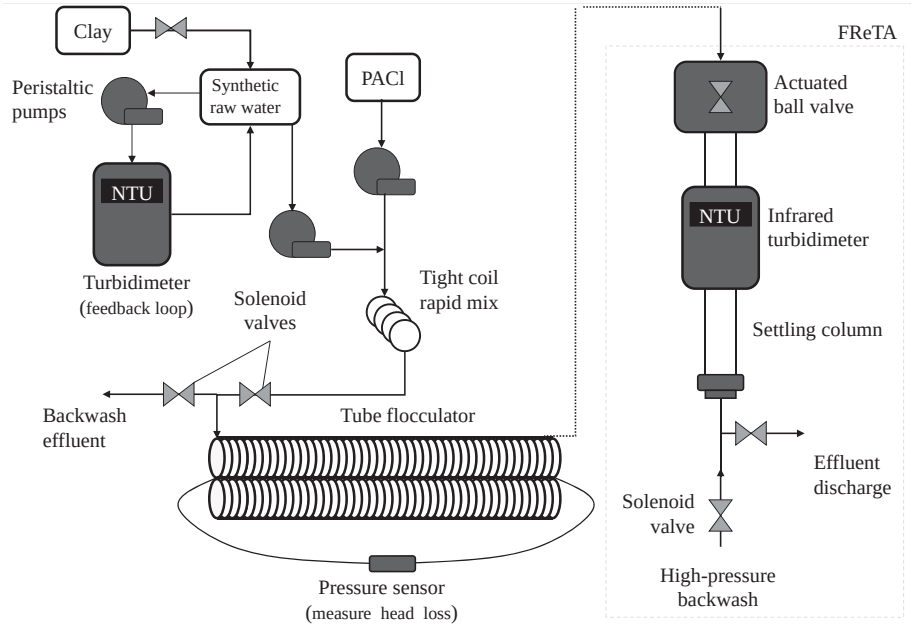

Figure 1: Schematic of the experimental assembly.

Briefly, the synthetic raw water (SRW) metering system consisted of a concentrated stock suspension of kaolinite clay (R.T. Vanderbilt Co., Inc., Norwalk, CT) mixed with tap water to produce a feedback-regulated constant turbidity raw water source (Weber-Shirk, 2008). Reported Cornell University tap water characteristics are: total hardness $150\,\frac{mg}{L}$ as $CaCO_3$, total alkalinity $121\,\frac{mg}{L}$ as $CaCO_3$, pH 7.6, aluminum $= 0\,to\,0.17\,\frac{mg}{L}$, and dissolved organic carbon $1.7\,\frac{mg}{L}$ Bolton Point Water System (2012). The concentrated clay stock and the SRW feedstock were each continuously stirred to ensure homogeneous suspensions. Influent turbidities of 5, 15, 50, 150, and 500 NTU were tested with both PACl and alum over a range of coagulant doses ($\sim 0.01 - 0.15\,mM\,Al$). All influent chemicals were metered with computer controlled Cole Parmer MasterFlex L/S digital peristaltic pumps. To better mimic coagulants used in water treatment practice, industry grade (31% as Al_2O_3) polyaluminum chloride (PACl), $(AlO_4Al_{12}(OH)_{24}(H_2O)_{12})^{7+}$ (Zhengzhou City Jintai Water Treatment Raw Material Co., Ltd.), and technical grade aluminum sulfate, $Al_2\,(SO_4)_3 \cdot 14.3H_2O$, (PTI Process Chemicals) were used as coagulants for all experiments. Each coagulant was diluted with distilled water to make the stock solutions.

The SRW and coagulant were passed through a rapid mix unit comprised of a $120\,cm$ segment of $4.3\,mm$ (0.17") ID tubing coiled around a cylinder with an outer diameter of 5

cm to ensure thorough mixing. Reynolds number in the rapid mix tube was approximately 1450. Results from a dye study showed that adequate mixing was achieved at this flow rate due to the secondary currents induced by the coiling.

The mixed coagulant and SRW entered a coiled tube flocculator ($56\,m$ or $84\,m$). The average velocity gradient in the flocculator, G, was maintained at $51\,s^{-1}$, calculated using relationships for laminar flow in coiled tubes described by Tse et al. Tse et al. (2011) (see equations 1-4 below). The overall plant flow rate, Q_{Plant}, was maintained at $5\,\frac{mL}{s}$ resulting in flocculator hydraulic residence times, of $800\,s$ and $1200\,s$ respectively. As Owen et al. Owen et al. (2008) note, flocculation is frequently studied in batch reactors with offline size measurements for aggregation processes, resulting in poor control over the energy dissipation rate, reaction time, and questionable size measurements. A tube flocculator was used in this research because it can be idealized as a high Peclet number reactor much like a baffled hydraulic flocculator and also because the average velocity gradient in laminar tube flow is well defined (Weber-Shirk and Lion, 2010).

After two hydraulic residence times in the flocculator, the flow was ramped to a stop, the FReTA actuated ball valve shown in Figure 1 closed, and the turbidity in the quiescent settling column was measured over a period of 30 minutes. FReTA was used to non-destructively measure both the sedimentation velocity and the residual turbidity of the effluent from the flocculator. The settling velocity of the particles was calculated by dividing the 13.6 cm distance between the bottom of the ball valve and the center of the zone illuminated by the turbidimeter's infrared LED by the time elapsed during settling. The residual turbidity was defined as the average settled turbidity in the fifty second interval around the selected capture velocity. Because turbidity was recorded continuously as the suspension settled, capture velocities between $2.7\,\frac{mm}{s}$ and $0.08\frac{mm}{s}$ can be specified when the data is analyzed.

Model

Conceptually, a successful flocculation model would determine effective collisions, collisions that result in particle aggregation, as a function of floc size for a given set of conditions. Since these parameters are not readily observable within a flocculator, measurable alternatives must be used. The dimensionless term $G\theta$ has been used as a measure of the collision potential provided by a flocculator that experiences laminar flow, where G is proportional to the rate of collisions and θ is the total time over which collisions occur (Cleasby, 1984). Equations 1 through 4 can be used to calculate G for a coiled flocculator, as described in Tse et alTse et al. (2011).

$$\bar{G} = \frac{64 Q_{Plant}}{3\pi d_{Tube}^3} \tag{1}$$

$$Re = \frac{4 Q_{Plant}}{\pi d_{Tube} \nu} \tag{2}$$

$$De = \sqrt{\frac{0.5 d_{Tube}}{R_{Bend}}} Re \tag{3}$$

$$G = \bar{G}\left(1 + 0.033 log(De)^4\right)^{0.5} \tag{4}$$

where: $\bar{G}$ is the average velocity gradient in a straight tube, Q_{Plant} is the plant flow rate, d_{Tube} is the diameter of the tube flocculator, Re is the Reynolds number, ν is the viscosity of water, De is the Dean number, and R_{Bend} is the radius of the coil in the flocculator. In laminar flow G is related to the energy dissipation rate , ε, by Equation 5. The experimental G of $51\,s^{-1}$ corresponds to $\varepsilon = 2.6\,\frac{mW}{kg}$.

$$\varepsilon = \nu G^2 \tag{5}$$

It is well known that not all collisions between suspended particles are effective, i.e., they do not all result in aggregation. Attachment efficiency, α, has been used to designate the fraction of collisions which result in aggregation. Unfortunately, α is not directly measurable or easily estimated. However, the fractional coverage of the colloid surface by coagulant can be estimated based on the geometric properties of the colloids and coagulant and is used here as an alternative for attachment efficiency. Given the influent clay concentration, $C_{Influent}$, the coagulant concentration, C_{PACl} or $C_{Al(OH)_3}$, and the coagulant aggregate size, d_{PACl} or $d_{Al(OH)_3}$, the number of coagulant aggregates per clay platelet can be calculated (see Equation 6). As an initial approximation, kaolin clay platelets were assumed to have the volume of a sphere with a diameter of $2\,\mu m$ (Ye et al., 2007; Lin et al., 2008). The platelets were assumed to be cylinders with a 10:1 diameter to height ratio, resulting in a diameter of $3.8\,\mu m$, height of $0.38\,\mu m$, and an initial surface area of $27\,\mu m^2$. PACl aggregate diameters were determined experimentally to be approximately $180\,nm$ (using a Malvern Zetasizer Nano-ZS). Amorphous $Al(OH)_3$ precipitate particles were estimated to be $100\,nm$ in diameter, but model calculations were not sensitive to this assumption (see discussion below). Since PACl is used as a coagulant by the Cornell water treatment plant, the solubility limit for aluminum was satisfied for the tap water entering the experimental system Bolton Point Water System (2012). The experiments used to create the model were performed over several months and the soluble aluminum concentration in the source water likely varied as indicated in the reported water characteristics ($0 - 0.17\,\frac{mg}{L}$), which may contribute to the spread of the data. As a result, the solubility limit was assumed to be satisfied and was not subtracted from the dose administered in experiments. However, this adjustment should be made in cases where the raw water has yet to be dosed with coagulant as is shown in Equation 6. Benshoten and EdzwaldBenschoten and Edzwald (1990) report the pH-dependent solubility of PACl and amorphous $Al(OH)_3$.

$$N_{perClay} = \frac{\left(C_{Coag} - C_{Coag(aq)}\right) V_{Clay}\rho_{Clay}}{\frac{\pi}{6} d_{Coag}^3 \rho_{Coag} C_{Influent}} \tag{6}$$

where $N_{perClay}$ is the number of coagulant aggregates per clay, C_{Coag} is the concentration of coagulant, $C_{Coag(aq)}$ is the solubility of the coagulant at the appropriate pH, V_{Clay} is the volume of a clay platelet, ρ_{Clay} is the density of clay, $2.65\,\frac{gm}{mL}$, d_{Coag} is the diameter of a coagulant aggregate, $d_{PACl} = 180\,nm$ and $d_{Al(OH)_3} = 100\,nm$, ρ_{Coag} is the density of the coagulant, $\rho_{PACl} = 1.138\,\frac{gm}{mL}$ based on laboratory measurement and $\rho_{Al(OH)_3} = 2.42\,\frac{gm}{mL}$ as reported by IPCSInternational Program on Chemical Safety (1998), and $C_{Influent}$ is the influent turbidity in $\frac{mg}{L}$. Turbidities were translated from NTU to $\frac{mg}{L}\,Clay$ using a conversion based on laboratory observations, $2\,\frac{mg}{L*NTU}$.

The above calculation of coagulant aggregates per clay colloid does not account for the possible attachment of coagulant to the walls of the experimental flocculation tube. In the bench-scale of laboratory experiments the inner surface of the flocculation tube can be a significant coagulant sink, a place where the coagulant will adhere and be removed from all subsequent processes. The fraction of coagulant aggregates that adhere to colloids in the suspension, R_{Clay}, (i.e. those that do not adhere to the flocculator tube wall) can be estimated by Equation 7.

$$R_{Clay} = \frac{SA_{ClayTotal}}{SA_{ClayTotal} + SA_{Wall}} \tag{7}$$

where SA_{Wall} is the surface area of the tube wall of the flocculator, $SA_{ClayTotal}$ is the surface area of all the clay colloids in a liquid volume equal to that of the flocculator (Equation 8). SA_{Wall} is a function of the length of flocculator tube, L_{Tube}, and the circumference of the flocculator tube, πd_{Tube} (Equation 10).

$$SA_{ClayTotal} = L_{Tube}\frac{\pi}{4}d_{Tube}^2 SA_{Clay} N_{Clay} \tag{8}$$

$$N_{Clay} = \frac{C_{Influent}}{\rho_{Clay} V_{Clay}} \tag{9}$$

$$SA_{Wall} = L_{Tube}\pi d_{Tube} \tag{10}$$

where $C_{Influent}$ is the raw water clay concentration, N_{Clay} is number of clay colloids per unit volume of suspension, and SA_{Clay} is the surface area of a single clay platelet.

After substitution, Equation 7 becomes:

$$R_{Clay} = \frac{SA_{ClayTotal}}{SA_{ClayTotal} + SA_{Wall}} = \frac{\frac{1}{4}d_{Tube} SA_{Clay} N_{Clay}}{\frac{1}{4}d_{Tube} SA_{Clay} N_{Clay} + 1} = \frac{1}{1 + \frac{4}{d_{Tube} SA_{Clay} N_{Clay}}} \tag{11}$$

The length of the flocculator tube drops out of the equation and thus the length of the zone where free coagulant aggregates are present is not needed to determine the distribution of the coagulant between the flocculator tube and the clay. The correction for wall losses expressed as fraction of coagulant available to react with clay is shown in Figure 2 as a function of influent turbidity.

Surface coverage of clay can also be reduced if coagulant particles stick to a clay surface that is already occupied by coagulant. A Poisson distribution was used to estimate the reduction in coverage due to coagulant aggregates stacking on top of one another instead of attaching to uncovered clay surface (Equation 12).

$$\Gamma = 1 - e^{\frac{-d_{Coag}^2}{SA_{Clay}} N_{perClay} R_{Clay}} \tag{12}$$

where SA_{Clay} is the surface area of a single clay platelet. A parallel analysis was performed using a random number generator to consecutively place each coagulant aggregate on a discretized grid. The ratio of occupied to total spaces on the grid gave an estimate of the fractional clay coverage that agreed with Equation 12. The effect of stacking is shown in Figure 3 and becomes significant at high coagulant doses.

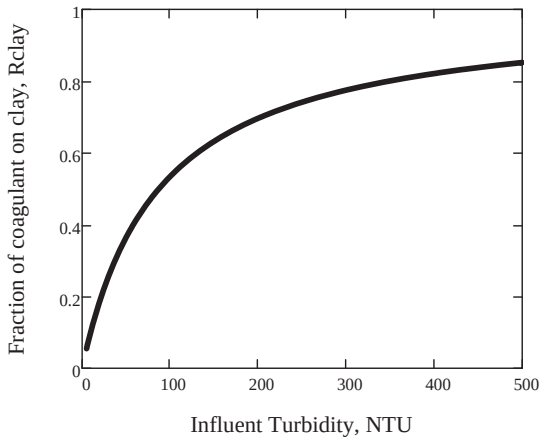

Figure 2: The fraction of coagulant aggregates that adhere to the surface of clay colloids in the experimental apparatus, R_{Clay}, as a function of influent turbidity

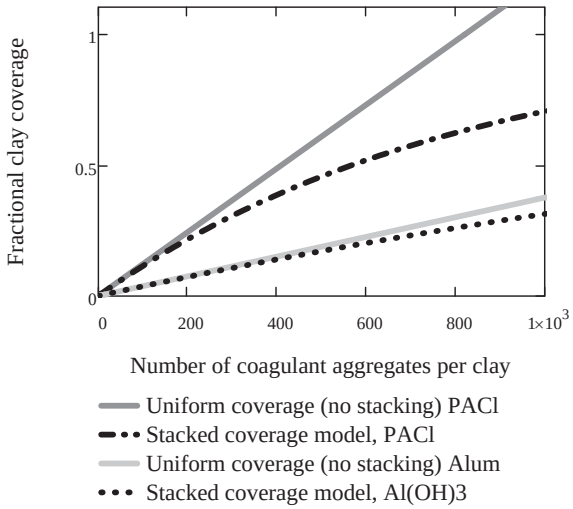

Figure 3: Fractional clay surface coverage for PACl and $Al(OH)_3$.

With quantifiable parameters for collisions provided by the flocculator ($G\theta$) and surface coverage (Γ) as a measure of the probability of attachment, the properties of the suspension must be incorporated into the model. The floc volume fraction, ϕ, gives the fraction of the volume of the suspension occupied by the combination of influent particles and precipitated coagulant. (Equation 13).

$$\phi = \frac{C_{Coag} R_{Clay}}{\rho_{Coag}} + \frac{C_{Influent}}{\rho_{Clay}} \tag{13}$$

The coagulant doses used in experiments contributed less than 2.5% to the floc volume fraction and thus Equation 13 can be simplified to:

$$\phi = \frac{C_{Influent}}{\rho_{Clay}} \tag{14}$$

In laminar flow flocculators the velocity between flocs scales with the average separation distance between flocs. The time between floc collisions is inversely proportional to ϕ and directly proportional to the velocity between flocs (or the separation distance or $\phi^{1/3}$). The result is that for laminar flow the average time for floc collisions scales with $\phi^{2/3}$ (Weber-Shirk and Lion, 2010).

Based on the above analysis, the product of the dimensionless model parameters, $G\theta\Gamma\phi^{2/3}$ was selected to characterize the number of effective collisions provided by a laminar flow tube flocculator. The dependent parameter of interest is the negative log of the fraction of clay particles remaining after the combined flocculation/sedimentation processes (Equation 15).

$$pC^* = -log\left(C^*\right) = -log\left(\frac{C_{Settled}}{C_{Influent}}\right) \tag{15}$$

where $C_{Influent}$ is the raw water clay concentration and $C_{Settled}$ is the settled water clay concentration after a settling time, $t_{Capture}$. In practice $t_{Capture}$ is set by the hydraulic residence time and geometry of the tube or plate settlers in the sedimentation tank. Experimentally $t_{Capture}$ was set in data analysis by the selection of a capture velocity, $V_{Capture}$ (Equation 16).

$$t_{Capture} = \frac{h_{column}}{V_{Capture}} \tag{16}$$

where h_{Column} is the distance between the top of the settling column and the point within the turbidimeter where turbidity was measured. Tse et al.Tse et al. (2011) provide a detailed description of analysis of the data acquired by FReTA.

The experimental results were first modeled by Equation 17 where m is the slope, and b is the intercept.

$$pC^* = m\,log\left(G\theta\Gamma\phi^{2/3}\right) + b \tag{17}$$

The fraction of clay particles remaining as residual turbidity was inversely proportional to $G\theta\Gamma\phi^{2/3}$ allowing the value of m to be set equal to 1. Using a slope of 1 for the model reduced the number of fitted parameters and did not significantly affect the model fit ($R^2 \geq 0.90$ for both PACl and alum). Equation 17 can be simplified to:

$$C^* = \left(\beta G\theta\Gamma\phi^{2/3}\right)^{-1} \tag{18}$$

where the coefficient, $\beta = 10^b$.

Results

The results from 136 experiments are shown in Figure 4 for a capture velocity of $0.12\,\frac{mm}{s}$ which is a conservatively designed lamellar settler capture velocity (Willis, 1978). The capture velocity is an input parameter to the data analysis model and model application can be generalized for a range of capture velocities between $0.1\,\frac{mm}{s}$ and $0.22\,\frac{mm}{s}$ as described below. The raw data for all influent turbidities, hydraulic residence times, and doses are shown in Figure 4 for both PACl and alum. The data has significant spread, but generally shows a

negative slope, indicating that increased coagulant dose is positively correlated to turbidity removal.

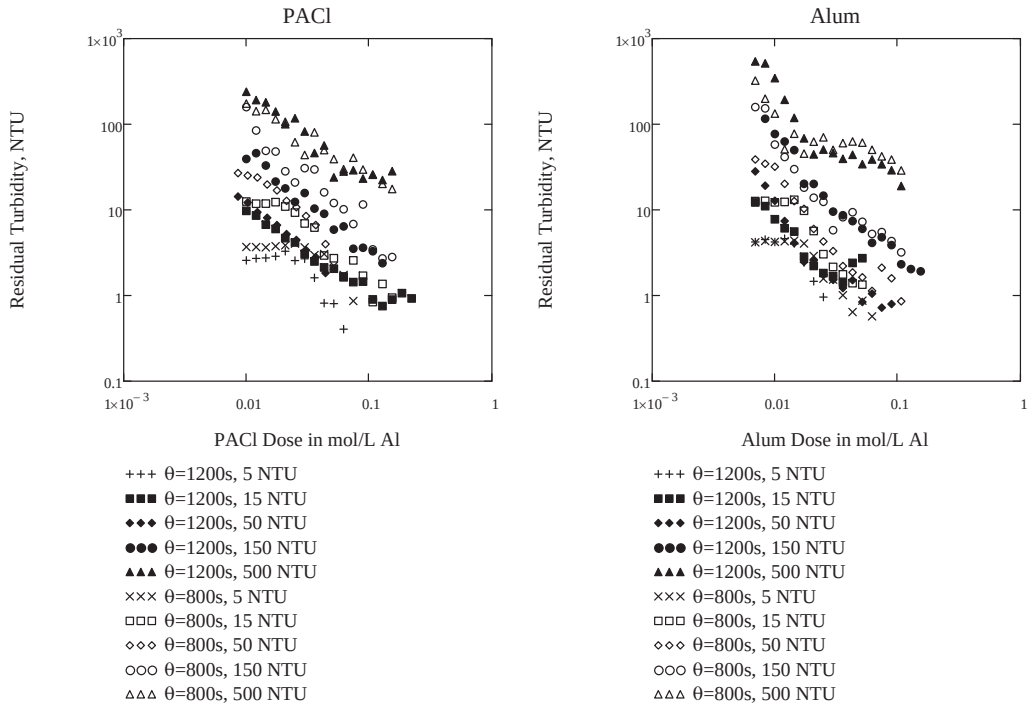

Figure 4: Residual turbidity as a function of coagulant dose for $V_{Capture} = 0.12\,\frac{mm}{s}$

Transforming the residual turbidity by Equation 15 aggregates the data and complicated trends are seen between the different influent turbidities (Figure 5). Given the same coagulant dose the highest removal efficiency is obtained by samples with turbidities of 50 and 150 NTU. Higher and lower influent turbidities both perform more poorly. This optimal influent turbidity suggests that there are two competing mechanisms that cause performance to worsen for both very high and very low influent turbidities. The two competing mechanisms at a constant coagulant dose are the fractional coverage of clay that decreases with increasing influent turbidity and the floc volume fraction that increases with influent turbidity.

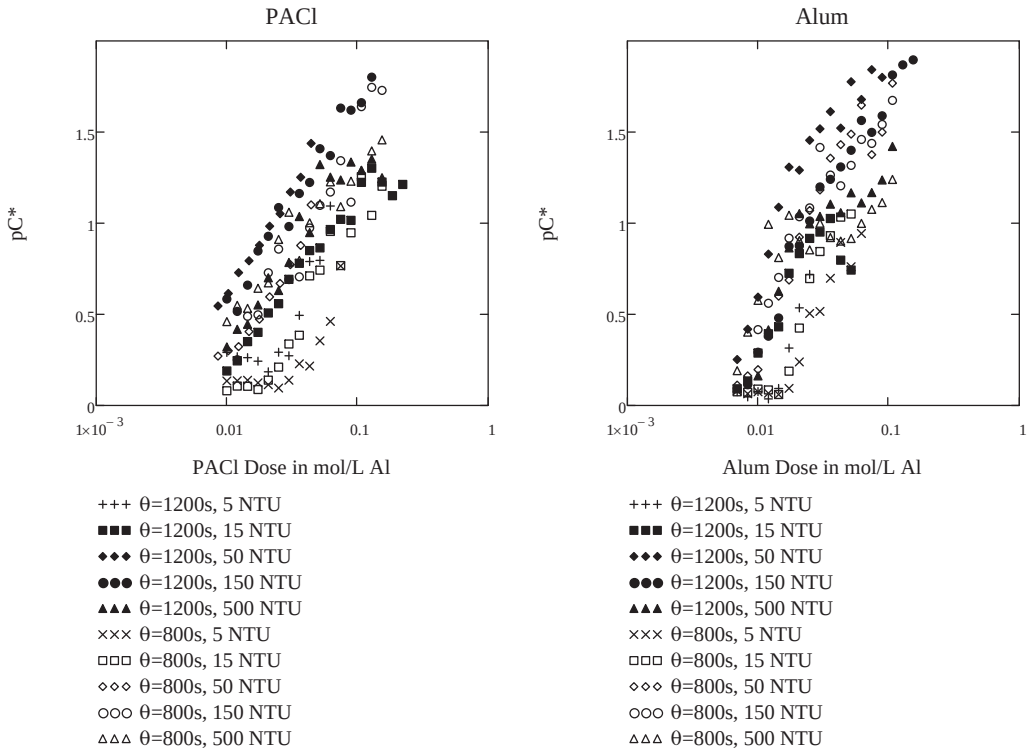

Figure 5: pC^* as a function of coagulant dose for $V_{Capture} = 0.12\,\frac{mm}{s}$

When the coagulant dose in Figure 5 was replaced with $G\theta\Gamma\phi^{2/3}$ from Equation 18 the data collapses to a narrow band indicating that the composite independent parameter, $G\theta\Gamma\phi^{2/3}$, captures a large fraction of the trends present in the data (see Figure 6). The coefficient β was fit to the data by using the mean of the intercept for the lines with slope of 1 defined by each data point The data for very low effective collision potential ($\Gamma G\theta\phi^{2/3} < 0.2$ for PACl and $\Gamma G\theta\phi^{2/3} < 0.12$ for alum) was removed before calculating β to eliminate suspensions that had insignificant sedimentation during the experimental settling time. The flocs created at such low effective collision potentials all have settling velocities lower than the capture velocity and negligible removal of turbidity was observed.

The data analysis outputs β for each selected capture velocity (Table 1). The relationship between β and capture velocity is shown in Figure 7 and was modeled very well by an equation of the form $\beta = \frac{\eta_{Coag}}{V_{Capture}}$ (Equations 19 and 20).

$$\beta_{PACl} = \frac{\eta_{PACl}}{V_{Capture}};\ R^2 = .999,\ N = 13 \tag{19}$$

$$\beta_{Alum} = \frac{\eta_{Alum}}{V_{Capture}};\ R^2 = .997,\ N = 13 \tag{20}$$

where $\eta_{PACl} = 0.49\,\frac{mm}{s}$ and $\eta_{Alum} = 0.818\,\frac{mm}{s}$. The lower bound of the capture velocity range was set by the duration of settling in the experiments, and the upper bound is likely set by the maximum sedimentation velocity of the flocs given the velocity gradient in the flocculator.

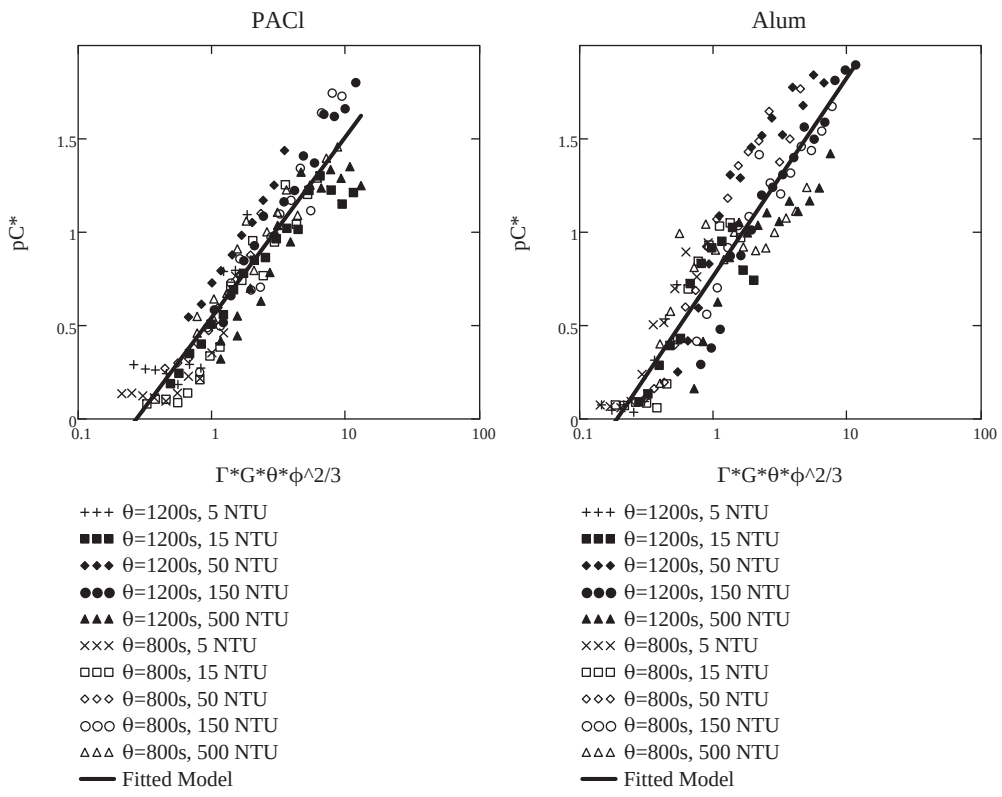

Figure 6: Model fit for pC^* as a function of effective collision potential for $V_{Capture} = 0.12\ \frac{mm}{s}$. Sample size, N, is 136 for PACl and 140 for Alum. $R^2_{PACl} = 0.92$ and $R^2_{Alum} = 0.89$.

To generalize the flocculation model within the range of tested capture velocities, Equations 19 and 20 were incorporated into Equation 18. Since surface coverage, Γ, is a function of the the coagulant dose , C_{Coag}, this relationship can be used to predict the dose required to reduce the settled water turbidity to a desired value for a sedimentation tank with a specified capture velocity (Equation 22). As an example, the PACl and alum doses required to achieve a settled turbidity of 3 NTU, a common influent turbidity for a rapid sand filter, are shown in Figure 8 for a range of influent turbidities and capture velocities.

$$C^* = \left(\frac{\eta_{Coag}}{V_{Capture}} G\theta\Gamma\phi^{2/3}\right)^{-1} \tag{21}$$

$$C_{Coag} = ln\left(1 - \left(\frac{C_{Influent}}{\frac{\eta_{Coag}}{V_{Capture}} C_{Settled}}\right) \frac{1}{G\theta} \left(\frac{\rho_{Clay}}{C_{Influent}}\right)^{\frac{2}{3}}\right) \frac{-d_{Coag}\pi\rho_{Coag}\left(1 + d_{Tube} SA_{Clay} \frac{C_{Influent}}{V_{Clay}\rho_{Clay}}\right)}{6d_{Tube}} + C_{Coag}(aq) \tag{22}$$

The model was validated by using it to predict residual turbidity for different experimental conditions than those used to obtain the model (i.e., different influent turbidity, velocity gradient, flocculation time, coagulant dose and capture velocity). The predicted residual turbidity and measured residual turbidity are compared in Figure 9.

Table 1: Correlation coefficient, R^2, and fitted parameter, β, for PACl and Alum as a function of capture velocity. Sample size, N, is 133 for PACl and 136 for Alum.

$V_{Capture}$	β_{PACl}	R^2_{PACl}	β_{Alum}	R^2_{Alum}
$0.1\,\frac{mm}{s}$	4.37	0.93	6.99	0.90
$0.12\,\frac{mm}{s}$	3.65	0.92	5.82	0.89
$0.14\,\frac{mm}{s}$	3.12	0.91	4.99	0.88
$0.16\,\frac{mm}{s}$	2.73	0.90	4.37	0.88
$0.18\,\frac{mm}{s}$	2.43	0.897	3.88	0.88
$0.2\,\frac{mm}{s}$	2.19	0.85	3.49	0.84
$0.22\,\frac{mm}{s}$	1.99	0.83	3.18	0.84

Discussion

A mechanistically-based hydraulic flocculation model has been created and validated for laminar flows. The form and parameterization of the model led to several useful findings. The influence of coagulant dose on flocculation performance can be explained by the fractional coverage of the colloid surface without regard for previously hypothesized coagulation mechanisms (charge-neutralization, electrostatic patch, sweep floc, etc). The change in required coagulant dose for the range of capture velocities embodied in the design of downstream sedimentation tanks is predictable and is incorporated into the flocculation model, increasing its flexibility and utility.

The flocculation model utilizes experimental observations obtained over wide operational ranges for many parameters. The inherent dimensionless relationships embodied in the model are mechanistic and the model fits are well-correlated to the data. The predictive capability of the model is excellent. The reader is cautioned that some model assumptions may not hold for all applications. While the PACl aggregate diameter was experimentally measured, the aluminum hydroxide aggregate diameter was estimated; $100\,nm$ was chosen to maximize the R^2 value for the model fit. However, the model is not sensitive to this input; changing the diameter of precipitated aluminum hydroxide to $50\,nm$ or $150\,nm$ only reduced the R^2 by 0.06.

In contrast to rapid sand filtration where pC^* is linearly proportional to filter depth, the flocculation model definitively shows that pC^* is directly proportional to the log of the effective collision potential $\left(log\left(\Gamma G\theta\phi^{2/3}\right)\right)$. While a particle in a sand filter has an equal probability of being removed in the first and last centimeter of the filter, colloids are much more likely to be incorporated into a floc in the first centimeter of the flocculator than in

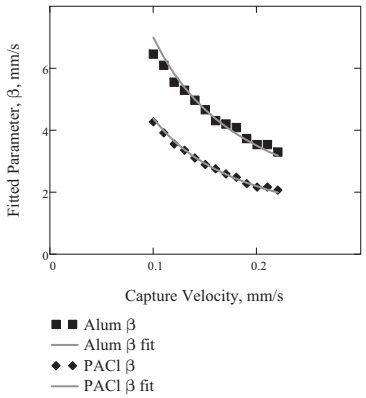

Figure 7: Model parameters as a function of capture velocity.

the last centimeter. Because flocs incorporate water as they grow, the floc volume fraction increases with floc size and the frequency of collisions increases. Thus, the proportion of collisions that result in aggregation, must decrease as flocs grow. Selective removal of colloids with high coagulant surface coverage is hypothesized to contribute to the diminishing rate of turbidity removal. The adhesive properties of the coagulant do not change, but as the colloids aggregate, the most adhesive surfaces are preferentially buried within the growing floc. Furthermore, due to the random distribution of coagulant aggregates to the surface of the colloids during coagulation, some statistical portion of the colloids will have a lower fractional surface coverage of coagulant. These colloids would be more likely to remain unaggregated in flocculation because their ability to adhere was lower.

The fitted parameter, η_{Coag}, has units of velocity, therefore it must be a function of parameters that give units of length per time. It is hypothesized that η_{Coag} may be proportional to the mean sedimentation velocity of the suspension after coagulation and flocculation. **?** describe the influence of G on final floc sedimentation velocity and observed that residual turbidity tends to decrease as G decreases. This relationship merits additional research.

The flocculation model provides a fundamental basis for the non-stoichiometric relationship between coagulant dose and the suspended solids concentration of the raw water. The five terms in flocculation equation set the interactions between raw water properties (ϕ and colloid surface area which contributes to Γ), coagulant size and dose (which also contribute to Γ), flocculator design ($G\theta$), and sedimentation tank design ($V_{Capture}$). In a given water treatment plant operating at constant flow rate the flocculator and sedimentation tank parameters are constant. An increase in turbidity causes an increase in ϕ, which improves C^*, and at constant coagulant dose causes a decrease in Γ, which decreases C^*. The competing influences of ϕ and Γ cause both very high and very low turbidity waters to be difficult to flocculate. High turbidity water is difficult to treat because the required coagulant dose becomes very large. Low turbidity water is hard to treat because ϕ is small and thus collisions are infrequent.

The important role of coagulant loss to reactor surfaces is characterized and provides insight into optimal flocculator geometry to reduce wall losses. Reactor geometry should minimize the surface area of the flocculator walls by using flow passages that are close to square. This is especially important for small scale hydraulic flocculators where distances

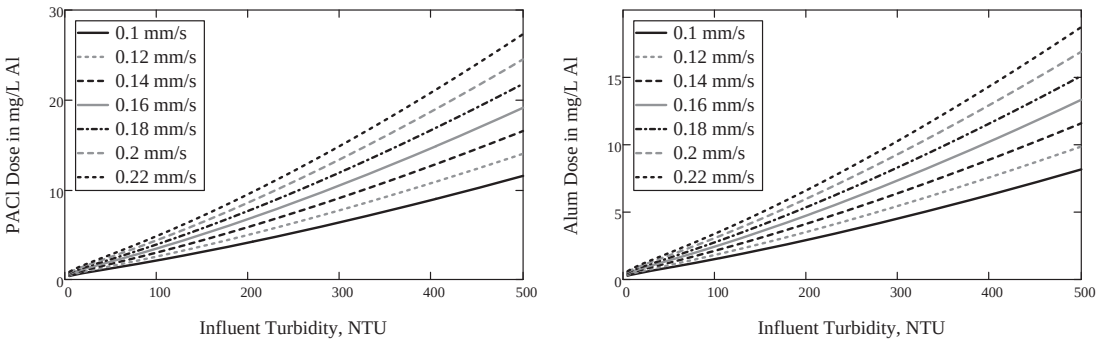

Figure 8: Model predictions using coagulant dose needed to achieve a settled turbidity of 3 NTU as a function of influent turbidity for a range of capture velocities. $\theta = 1200\,s$, $C_{Settled} = 3\,NTU$.

between flocculator baffles are reduced and coagulant loss is more significant.

The form of the model indicates that increasing the residence time in the flocculator leads to quantifiable improvements in performance or a reduction in the coagulant demand. This information can be used to optimize reactor design, minimize costs, and forecast chemical costs. While not the focus of this study, the influence of sedimentation tank capture velocity on required coagulant dose is depicted in Figure 8. With this information, capture velocity can be chosen in the same way that hydraulic residence time in the flocculator can be chosen, by comparing construction costs and site considerations to coagulant costs.

It is noteworthy that the predictive success of the model is achieved without incorporating the charge of the colloids or coagulant. The lack of a stoichiometric relationship between raw water turbidity and required coagulant dose in these experiments suggested that surface charge neutralization was not a controlling factor in flocculation. There are also reports in the literature where successful flocculation has been achieved when particle surface charge had not been neutralized (Gao et al., 2005; Chu et al., 2008; Wu et al., 2007). The experimental data do not provide any evidence of a shift in particle removal that could be attributed to charge neutralization, as this effect would be expected to be reflected by a large incremental change in pC^* over a small incremental change in coagulant dose where charge neutralization occurs. In addition no decrease in pC^* was observed at high coagulant dose, as would be expected with charge reversal. Thus, inclusion of surface charge in the model was not justified by the data.

The model is a powerful predictor of flocculation behavior under the tested conditions. Further tests should be done to expand the reach of the model from laminar flow (bench-scale)

a)

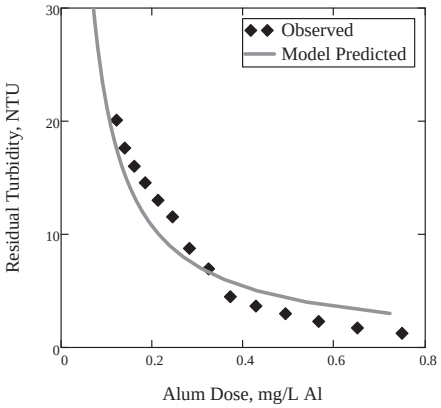

b)

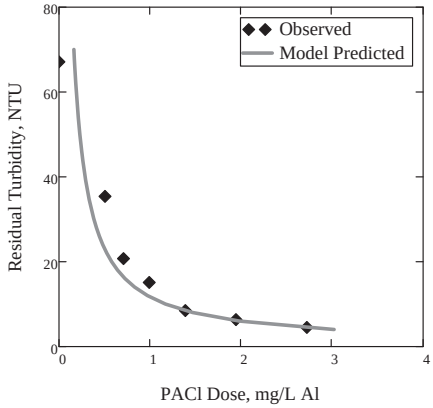

Figure 9: Model validation using a) alum, $C_{Influent} = 30\,NTU$, $\theta = 1087\,s$, $G = 57.2\,s^{-1}$ for $V_{Capture} = 0.10\,\frac{mm}{s}$. $R^2 = 0.97$ and b) PACl, $C_{Influent} = 75\,NTU$, $\theta = 997\,s$, and $G = 63.3\,s^{-1}$ for $V_{Capture} = 0.22\,\frac{mm}{s}$. $R^2 = 0.99$

flocculators to turbulent flow (field-scale) hydraulic flocculators. It is expected that the same mechanistic relationships will be present with the exception of G which is not expected to characterize turbulent flow flocculation. Flocculator properties characterized by G in laminar flow can be described by $\varepsilon^{1/3}$ in turbulent flow Weber-Shirk and Lion (2010). Similarly, natural waters with varying water chemistry and colloid types should be tested to elucidate the impact of natural organic matter, pH, and alkalinity on flocculation performance. The importance of surface area as a coagulant sink suggests that small diameter particulate matter would be significant sinks for coagulant. In addition, complexation of added coagulant by natural dissolved organic matter can also act as a coagulant sink and increase the required dose. It is reasonable to believe that with additional testing this model could be the basis for flocculation design and operation for a wide range of hydraulic flocculators and source waters. Mechanistically based predictive models for flocculator design and operation are possible and merit further development for synthesis into scalable guidelines for engineers and plant operators.

Acknowledgments

The research described in this paper was funded by the San Juan Foundation. This project was supported by a number of people at Cornell University, including Paul Charles, Timothy Brock, Alexander Krolick, Michael Adelman, Craig Bullington, and Dale Johnson.

References

Akers, R., Rushton, A., Stenhouse, J., 1987. Floc breakage: The dynamic response of the particle size distribution in a flocculated suspension to a step change in turbulent energy

dissipation. Chem. Eng. Sci. 42 (4), 787 – 798.
URL http://www.sciencedirect.com/science/article/pii/0009250987800386

Benschoten, J. E. V., Edzwald, J. K., 1990. Chemical aspects of coagulation using aluminum salts - i. hydrolytic reactions of alum and polyaluminum chloride. Water Res. 24 (12), 1519–1526.
URL http://dx.doi.org/10.1016/0043-1354(90)90086-L

Bolton Point Water System, 2012. Drinking water quality report. Tech. rep., Southern Cayuga Lake Intermunicipal Water Commission.

Chu, Y. B., Gao, B. Y., Yue, Q. Y., Wang, Y., 2008. Investigation of dynamic processing on aluminum floc aggregation: Cyclic shearing recovery and effect of sulfate ion. Sci. China, Ser. B: Chem. 51, 386–392, 10.1007/s11426-007-0129-2.
URL http://dx.doi.org/10.1007/s11426-007-0129-2

Cleasby, J., 1984. Is velocity gradient a valid turbulent flocculation parameter? J. Environ. Eng. (Reston, VA, U. S.) 110 (5), 875–897.

Gao, B. Y., Chu, Y. B., Yue, Q. Y., Wang, B. J., Wang, S. G., 2005. Characterization and coagulation of a polyaluminum chloride (PAC) coagulant with high Al13 content. J. Environ. Manage. 76 (2), 143–147.

Hendricks, D. W., 2006. Guidelines and Criteria for Design. Water treatment unit processes: physical and chemical. CRC Press: Taylor and Francis Group.

International Program on Chemical Safety, 1998. Aluminum hydroxide.

Kawamura, S., 1991. Integrated design of water treatment facilities. Wiley, New York.

Lin, J.-L., Chin, C.-J. M., Huang, C., Pan, J. R., Wang, D., 2008. Coagulation behavior of Al13 aggregates. Water Res. 42 (16), 4281–4290.
URL http://dx.doi.org/10.1016/j.watres.2008.07.028

Owen, A. T., Fawell, P. D., Swift, J. D., Labbett, D. M., Benn, F. A., Farrow, J. B., 2008. Using turbulent pipe flow to study the factors affecting polymer-bridging flocculation of mineral systems. Int. J. Miner. Process. 87 (3-4), 90–99.

Schulz, C. R., Okun, D. A., 1984. Surface Water Treatment for Communities in Developing Countries. John Wiley and Sons Inc., Great Britain.

The Great Lakes - Upper Mississippi River Board of State and Provincial Public Health and Environmental Managers, 2007. Recommended standards for water works. Tech. rep., Health Research Inc.

Tse, I. C., Swetland, K., Weber-Shirk, M. L., Lion, L. W., 2011. Method for quantitative analysis of flocculation performance. Water Res. 45 (10), 3075–3084.

Weber-Shirk, M. L., 2008. An automated method for testing process parameters.

Weber-Shirk, M. L., Lion, L. W., 2010. Flocculation model and collision potential for reactors with flows characterized by high peclet numbers. Water Res. 44 (18), 5180–5187.

Willis, R. M., 1978. Tubular settlers-a technical review. J. - Am. Water Works Assoc. June, 331–335.

Wu, X., Ge, X., Wang, D., Tang, H., 2007. Distinct coagulation mechanism and model between alum and high Al13-PACl. Colloids Surf., A 305 (1-3), 89–96.

Ye, C., Wang, D., Shi, B., Yu, J., Qu, J., Edwards, M., Tang, H., 2007. Alkalinity effect of coagulation with polyaluminum chlorides: Role of electrostatic patch. Colloids Surf., A 294 (1-3), 163–173.
URL http://dx.doi.org/10.1016/j.colsurfa.2006.08.005